GEOLOGICAL SURVEY OF CANADA
OPEN FILE 7853

Targeted Geoscience Initiative 4: Contributions to the Understanding of Volcanogenic Massive Sulphide Deposit Genesis and Exploration Methods Development

LA-ICP-MS analysis of volatile trace elements in massive sulphides and host rocks of selected VMS deposits of the Bathurst Mining Camp, New Brunswick: methodology and application to exploration

Azam Soltani Dehnavi, David R. Lentz, and Christopher R.M. McFarlane

[1]University of New Brunswick, Fredericton, New Brunswick

2015

Recommended citation

Soltani Dehnavi, A., Lentz, D.R., and McFarlane, C.R.M., 2015. LA-ICP-MS analysis of volatile trace elements in massive sulphides and host rocks of selected VMS deposits of the Bathurst Mining Camp, New Brunswick: methodology and application to exploration, *In:* Targeted Geoscience Initiative 4: Contributions to the Understanding of Volcanogenic Massive Sulphide Deposit Genesis and Exploration Methods Development, (ed.) J.M. Peter and P. Mercier-Langevin; Geological Survey of Canada, Open File 7853, p. 59–80.

Publications in this series have not been edited; they are released as submitted by the author.

Contribution to the Geological Survey of Canada's Targeted Geoscience Initiative 4 (TGI-4) Program (2010–2015)

TABLE OF CONTENTS

Tables

LA-ICP-MS analysis of volatile trace elements in massive sulphides and host rocks of selected VMS deposits of the Bathurst Mining Camp, New Brunswick: methodology and application to exploration

Azam Soltani Dehnavi*, David R. Lentz†, and Christopher R.M. McFarlane‡

Department of Earth Sciences, University of New Brunswick, Fredericton, New Brunswick E3B 5A3
*Author's e-mail: azam.soltani@unb.ca
†Author's e-mail: dlentz@unb.ca
‡Author's e-mail: crmm@unb.ca

ABSTRACT

The application of volatile trace element contents of pyrite, chlorite, and white mica in selected polymetallic Zn-Pb-Cu-Ag volcanogenic massive sulphide (VMS) deposits of the Bathurst Mining Camp, northern New Brunswick (Armstrong A, Brunswick No. 12, Canoe Landing Lake, Halfmile Lake Deep Zone, Key Anacon, Louvicourt, and Restigouche) as a vectoring tool in VMS exploration has been investigated. In situ volatile trace element contents (As, Cd, Hg, In, Sb, Tl, etc.) were determined by laser ablation inductively coupled plasma mass spectrometry (LA-ICP-MS). Pyrite is a ubiquitous sulphide in altered host rocks to VMS mineralization and can accommodate a wide range of volatile trace elements. Most analyzed pyrite grains are arsenian with As contents up to 7.3 wt%, Sb (up to 2910 ppm), Tl (up to 4110 ppm), Au (up to 73.2 ppm), Hg (up to 220 ppm), In (up to 49 ppm), and Cd (up to 270 ppm). Variations in the spot chemical compositions of pyrite in stratigraphic profiles of the examined deposits reveal distinct volatile trace element features. Pyrite in the footwall alteration zones typically displays systematically increasing volatile trace element contents with decreasing distance stratigraphically upward to the ore horizon. However, in the hanging-wall alteration zones, there are no consistent pyrite chemical compositional trends. Pyrite in the hanging wall of some deposits, such as Brunswick No. 12, Canoe Landing Lake, Restigouche, and Key Anacon, show high As in the upper portions and, to a lesser extent, higher abundances of other volatile trace elements. Volatile element contents of chlorite and white mica (muscovitic to phengitic in composition) indicate that these elements are crystal lattice-bound. White mica typically contains As (up to 1.01 wt%), Sb (up to 4750 ppm), Tl (up to 698 ppm), In (up to 563 ppm), Hg (up to 67 ppm), Cd (up to 83 ppm), and Bi (up to 185 ppm). In comparison to white mica, chlorite is preferentially enriched in Cd (0.07–420 ppm) and Bi (0.02–185 ppm). The spot LA-ICP-MS analyses of chlorite and white mica demonstrate that volatile trace element contents of hanging-wall- and footwall-altered rocks increase with decreasing distance toward mineralization.

Our data indicate that pyrite, chlorite, and white mica are the residence sites of significant abundances of volatile trace elements, in particular As, Sb, Tl, Bi, and to lesser extent Cd, In, and Hg. Therefore, these minerals can serve as the primary widespread dispersal proxies for volatile elements in the studied drillholes. Systematic trends in volatile trace element distribution patterns in pyrite, chlorite, and white mica can be used to vector toward VMS mineralization in the Bathurst Mining Camp. This methodology may be applicable in other areas where polymetallic deposits occur, and may complement other geochemical and geophysical exploration methods.

INTRODUCTION

The world-class Zn-Pb-Cu-Ag volcanogenic massive sulphide (VMS) deposits of the Bathurst Mining Camp (BMC), northern New Brunswick, are hosted by Middle Ordovician bimodal volcanic and sedimentary rocks, which have undergone complex polyphase deformation and associated lower- to upper-greenschist- and locally blueschist-facies regional metamorphism. Deformation and metamorphism occurred primarily during closure of the Tetagouche-Exploits back-arc basin in the Late Ordovician to Early Silurian (Salinic Orogeny) and Late Silurian Acadian Orogeny (Goodfellow and McCutcheon, 2003).

The volatile trace elements of interest in this study belong to the siderophile element group (As, Sb, Tl, and Bi) and the chalcophile element group (Cd, Hg,

Soltani Dehnavi, A., Lentz, D.R., and McFarlane, C.R.M., 2015. LA-ICP-MS analysis of volatile trace elements in massive sulphides and host rocks of selected VMS deposits of the Bathurst Mining Camp, New Brunswick: methodology and application to exploration, *In:* Targeted Geoscience Initiative 4: Contributions to the Understanding of Volcanogenic Massive Sulphide Deposit Genesis and Exploration Methods Development, (ed.) J.M. Peter and P. Mercier-Langevin; Geological Survey of Canada, Open File 7853, p. 59–80.

and In). The volatile trace elements, particularly Hg, are potential pathfinders (lithogeochemical vectors within bounding host rocks) in geochemical prospecting for a wide variety of base- and precious-metal deposits. Primary and secondary dispersion haloes of volatile trace elements can be used for detecting buried mineralization (Ryall, 1981; Carr et al., 1986). The distributions of some volatile trace elements in VMS deposits of the BMC deposits have been reported previously (Goodfellow, 1975; Chen, 1978; Jambor, 1979, 1981; Luff et al., 1992; Lentz and Goodfellow, 1993, 1996; Lentz et al., 1997; Goodfellow and McCutcheon, 2003; McClenaghan et al., 2003, 2004, 2006, 2009; Peter et al., 2003a,b; McLellan et al., 2006; Walker and Lentz, 2006). The contents of these elements have been shown to be highly variable among the four time-stratigraphic ore horizons (Stratmat, Brunswick, Caribou, and Chester) in the BMC (Goodfellow and McCutcheon, 2003). The whole-rock analyses of Louvicourt samples exhibit atypically high contents of volatile elements Sb, Hg, and Tl (McClenaghan et al., 2006). The contents of some volatile trace elements in sulphides from the Brunswick No. 12 deposit have been previously determined by laser ablation inductively coupled plasma mass spectrometry (LA-ICP-MS) (McClenaghan et al., 2009). The volatile element contents of sedimentary rocks in the BMC have also previously been reported (Peter et al., 2003a,b). To date, however, there has been no comprehensive volatile trace element assessment of sulphide and silicate minerals in the BMC.

Herein we present a synopsis of the volatile trace element characterization of representative major deposits of the BMC (Armstrong, Brunswick No. 6 and No. 12, Caribou, Canoe Landing Lake, Halfmile Lake deep zone, Heath Steele B zone, Key Anacon, Louvicourt, and Restigouche). The deposits were selected based on their geological and exploration significance and because they have been previously well sampled and described. The volatile element composition of pyrite (the most abundant disseminated sulphide mineral in the stratigraphic footwall and hanging wall of the deposits), chlorite and white mica (muscovitic to phengitic in composition) were analyzed by LA-ICP-MS. This technique provides in situ measurement capabilities, high spatial resolution sampling, low detection limits, use of standard polished thin sections (no special sample preparation required), and cost efficiency (hundreds of analyses per day). The methodology development included an assessment of optimized ablation conditions, choice of external and internal standards, and data-reduction strategies.

The main objectives of this study are (1) to present the optimal methodology for analyzing volatile trace element contents of pyrite, chlorite, and white mica by LA-ICP-MS; (2) to characterize hydrothermal up-flow zones in studied drillholes in order to discriminate samples that are proximal to the sulphide horizons from those more distal (i.e. dispersion haloes); (3) to present mineral (sulphides and silicates) geochemical exploration vectoring tools that can be applied specifically to the BMC and to present approaches that can be used elsewhere.

METHODOLOGY

Optical Microscopy

Detailed optical microscopic (reflected and transmitted light) examination of polished thin sections is a prerequisite to in situ LA-ICP-MS analysis of pyrite and phyllosilicate minerals. Since LA-ICP-MS is a destructive technique, imaging of the samples prior to analysis is required. The fine-grained nature of the samples that were investigated in this study necessitated documentation of mineral textures and their relationship with coexisting phases. In order to yield meaningful results, sampling points (ablation spots) were selected to preclude sampling multiple phases simultaneously or phases with visible inclusions. Although inclusions may occur in subsurface at the micro- to nano-scale within the volume of material ablated, the former is readily detectable in the laser ablation time-series and can subsequently be omitted from the integrated spectra.

Laser Ablation Inductively Coupled Plasma Mass Spectrometry

The analyses were performed in the Department of Earth Sciences, University of New Brunswick, using a Resonetics Resolution™ M-50 193 nm ArF (excimer) laser system connected to an Agilent 7700X quadrupole inductively coupled plasma mass spectrometer (Q-ICP-MS) equipped with dual external rotary pumps. The instruments have a dedicated high-capacity (up to 20 L/min) Hg trap on all of the gas lines that enter the laser and ICP-MS. This allowed background ^{202}Hg gas to remain <1200 count per second (cps) under the highest sensitivity conditions. Modifications to standard analytical protocols were required in this study, and this included an assessment of optimized ablation conditions (laser sampling and energy density), choice of external and internal standards, and data-reduction strategies.

Analyses of pyrite were carried out in spot mode, and laser crater diameters of 17, 24, and 33 μm were selected on the basis of textural criteria, thickness of the polished sections, and necessary analytical precision and detection limits. The laser was operated at a repetition rate of 3 or 4 Hz, with the laser fluence held at ~1 J/cm^2 (see Table 1 for more information about the instrument operating conditions). Standard-sample

Table 1. Operating conditions for the LA-ICP-MS instrumentation used in this study.

ICP MS Agilent 7700x tuning	
RF power	1550 W
Torch depth	5.0 mm
Oxide production	ThO^+/Th^+ <0.3%
Double-charged production	$^{22}M^{++}/44Ca^+$ <0.3%
Ionization efficiency	$^{238}U^+/^{232}Th^+$ ~1.05

Laser ablation Resonetics S-155	
Type	193 nm excimer (20 ns pulse)
	LA condition for sulphides
Crater diameter	17-24-33 µm
Repetition rate	4-3 Hz
Fluence	~1 J/cm^2
Background time	40–120 s
Ablation time	40 s
Total time per spot	1.3–2.7 min
In-cell gas carrier	350 mL/min He and 960 mL/min Ar
N_2	2.0 mL/min
Type	LA condition for silicate
Crater diameter	66 µm
Repetition rate	4 Hz
Fluence	~1 J/cm^2
Background time	40 s
Ablation time	40 s
Total time per spot	80 s
In-cell gas carrier	325 mL/min He 960 mL/min Ar
N_2	2.0 mL/min

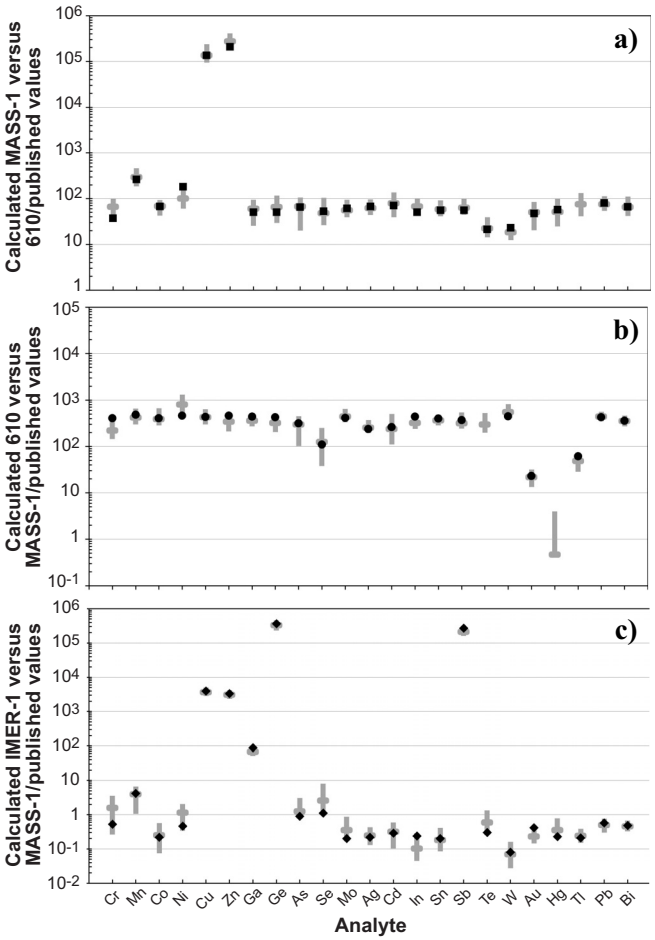

Figure 1. Assessment of the accuracy of data obtained from calculation of standards (MASS-1, NIST610, and IMER-1) analyzed along with pyrite samples. The average calculated values are compared to the published values for each standard. Plots show similar values for most of the elements. Internal standardization was obtained from the data published for the MASS-1, NIST610 (Fe), and IMER-1 (S) standards. Grey bars show the range of the examined elements (minimum and maximum).

bracketing and external calibration was performed using USGS MASS-1 (Wilson et al., 2002). For quantification of pyrite, Fe was selected as the internal standard (stoichiometric value). Data deconvolution was done offline using the Iolite™ 2.5 trace element data reduction scheme (Paton et al., 2011). Iolite has the ability to visualize the ion beam intensities against time and select portions of ablated signals to avoid transient signals related to inclusions or other heterogeneities. We also demonstrated that matrix-mismatching effects, such as using NIST610 (a Ca-Na-Si glass) as a standard to calculate element contents in MASS-1, were not a significant problem.

The MASS-1 standard was analyzed over 300 times over the course of one year and its calibration against NIST610 glass, using Fe as the internal standard, yielded average values that are close to the published values (Fig. 1a; Table 2). By analogy, under the same analytical conditions, the average contents obtained for NIST610 standardized against MASS-1, again using Fe as the internal standard, displayed very close correspondence to the reported values (Fig. 1b; Table 2). By using this approach, a wider calibration range is attained, and elements for which no certified values exist (such as Hg and Te in NIST610 glass, and Tl in MASS-1) can be rigorously assessed (Table 3). The informational values were added to the standard definitions (Soltani Dehnavi et al., 2014e).

The fine-grained nature of the chlorite and white mica and the presence of fine-grained quartz and pyrite, especially in association with white mica, made selection of ablation spots critically important (Fig. 2). One of the important features of LA-ICP-MS analysis is the ability to determine whether the elements occur in the mineral lattice or within micro-inclusions of other minerals. Lattice substitution of volatile trace elements in chlorite and white mica is indicated by the presence of a flat profile in the single-spot LA-ICP-MS data (Fig. 3). A beam diameter of 66 µm was used for spot analyses of chlorite and white mica. Silicon (stoichiometric values) was selected as the internal standard for quantification of white mica and chlorite. Data were corrected using NIST610 as an external standard. There are no certified Hg and Te values reported for

Table 2. Summary of obtained compositional variations of MASS-1, NIST 610, and IMER-1 in this study (ppm).

	Calculated NIST 610_Fe (n>300)				**Calculated MASS-1_Fe** (n>300)				**Calculated IMER-1 vs. MASS1_S** (n=60)			
Analyte	Min	Mean	Max	Published	Min	Mean	Max	Published	Min	Mean	Max	Suggested
Cr	165	224	380	405	41.9	67.3	89	37	0.31	1.62	3	0.53
Mn	337	423	580	485	212	298	405	260	1.25	4.05	5.6	4.20
Co	325	394	590	405	48	69.3	82.7	67	0.09	0.26	0.48	0.22
Ni	640	806	1160	459	68.4	102	125	180	0.4	1.16	1.73	0.46
Cu	338	428	560	430	107100	137102	209000	134000	3349	3695	4310	3930
Zn	241	346	429	456	202000	278297	361800	207383	2755	3150	3540	3328
Ga	310	361	465	438	29.1	60.7	83.1	50	60.6	68.4	82	87.8
Ge	232	324	430	426	33.7	66.0	102	50	276900	337552	383900	365500
As	115	300	396	317	22.8	67.9	93	65	BDL	1.25	2.6	0.90
Se	43	126	220	109	30	48.6	92	53	BDL	2.63	6.8	1.12
Mo	375	444	570	410	44.6	56.7	83	61	BDL	0.36	0.74	0.20
Ag	221	257	328	239	50.1	63.3	85	67	0.15	0.25	0.36	0.22
Cd	125	242	440	259	44.7	80.7	120	70	0.12	0.33	0.50	0.29
In	270	323	377	441	53.6	68.3	87.1	50	0.05	0.10	0.16	0.24
Sn	321	371	429	396	47.1	59.0	81	55	0.1	0.19	0.35	0.20
Sb	276	318	480	369	50.5	64.4	89.2	55	189600	216600	257200	269200
Te	224	302	460		16.4	22.4	34.5	21	BDL	0.60	1.12	0.30
W	468	552	720	445	14.2	18.6	22.7	23	0.03	0.07	0.14	0.08
Au	15.1	21.9	28.2	23	23.0	51.1	74	47	0.17	0.24	0.29	0.42
Hg	BDL	0.47	3.5		28.1	52.0	89	57	BDL	0.36	0.67	0.23
Tl	32.4	49.2	60.1	61	46.7	76.2	116		0.18	0.25	0.33	0.21
Pb	405	449	494	426	61.5	76.4	99.7	80	0.36	0.51	0.64	0.58
Bi	310	359	409	358	47.3	66.3	98	66	0.39	0.47	0.56	0.48

NOTE: BDL = below detection limit

NIST610; therefore, as described above, the informational values of NIST610 established as part of this study were used (Table 3) Table 1 contains additional information about the operating conditions of the instrument (Soltani Dehnavi et al., 2014f).

Accuracy and Precision

To evaluate the accuracy of the analyses, the element contents of each standard and pyrite were analyzed, the data reduced, and the results were compared to the published values; MASS-1 was calibrated against the external standard NIST610 and vice versa (Table 2). Iron was selected as an internal standard based on published values for each standard ($Fe_{MASS\text{-}1}$=15.6 wt% and $Fe_{NIST610}$=0.045 wt%). The average values obtained are in good agreement with the published data (Fig. 1a,b). In order to assess the reproducibility of this methodology, results obtained for IMER-1 (as consistency standard) were compared to the suggested values (see Ding et al., 2011). Element values for IMER-1 were then calculated against MASS-1 using S as the internal standard. The results demonstrate an acceptable degree of consistency and reproducibility with a range of accuracy and precision of less than 10% for most elements (Fig. 1c, Table 2). The relationships between the calculated values for standards and published values are shown in binary plots in Figure 4, with the best agreement for IMER-1 and MASS-1, whereas the poorest agreement is with NIST610.

Data quality monitoring for phyllosilicate minerals was conducted using the approach described above. NIST610 was calibrated against the external standard

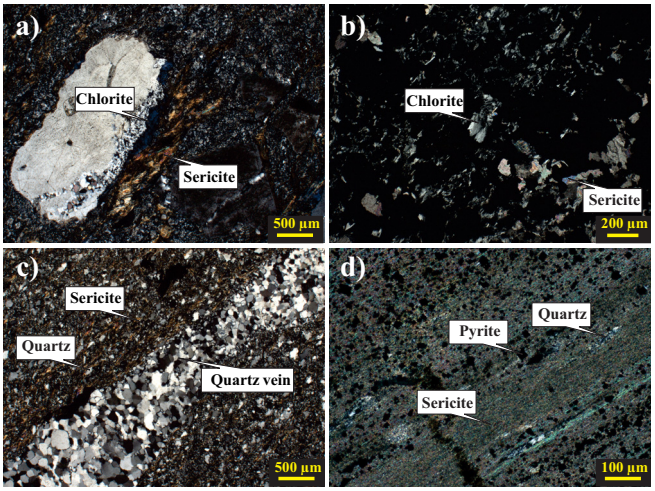

Figure 2. Photomicrographs (crossed-polars) of representative host-rock samples from the BMC. **a)** Fe-chlorite (chlorite) and white mica (sericite) (drillhole HN-119 @ 308': Halfmile Lake Deep Zone deposit); **b)** Mg-chlorite (chlorite) and white mica (sericite) together with sulphides (black colour) in a semi-massive sulphide sample (drillhole KA 93-42 @ 423 m: Key Anacon deposit); **c)** Fine-grained matrix composed of white mica (sericite) and quartz (drillhole HN-119 @ 617': Deep Zone, Halfmile Lake deposit); and **d)** white mica (sericite) band with disseminated fine-grained pyrite (sample from drillhole LGF-6 @ 210': Louvicourt deposit).

Table 3. Informational values for unreported elements that are calculated in this study for standards MASS-1 and NIST 610.

	Standards (ppm)	
Element	MASS-1	NIAT 610
Hg		0.47
Te		297
Tl	68.3	

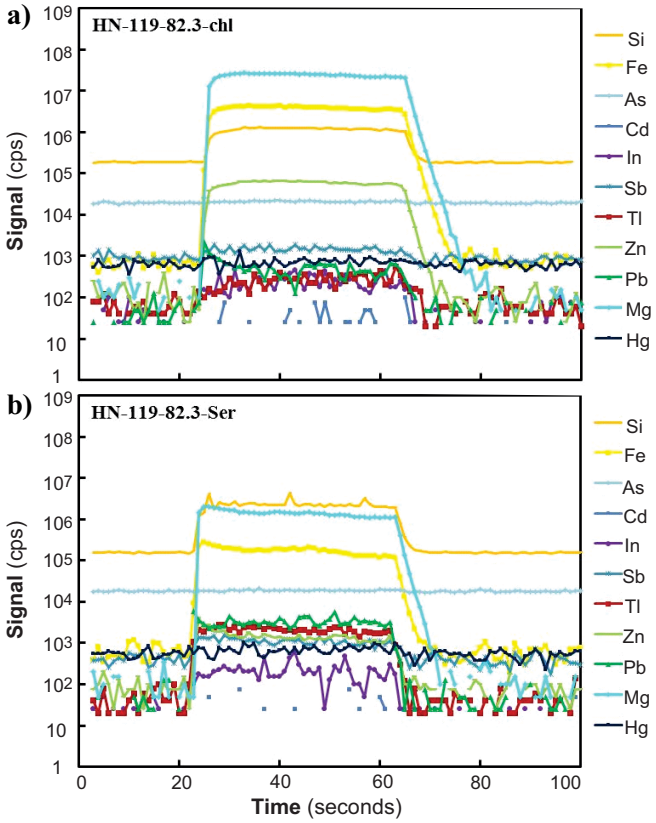

Figure 3. Raw count data (counts per seconds) for selected elements plotted as a function of time for a single-spot LA-ICP-MS for **(a)** chlorite and **(b)** white mica from the Halfmile Lake Deep Zone deposit, Bathurst Mining Camp.

NIST612 and vice versa, using published values for Si as the internal standard ($Si_{NIST610}$=32.7 wt% and $Si_{NIST612}$=33.6 wt%) (Table 4). The results demonstrate a good agreement between the values obtained in this study and data published for the standards (Fig. 5).

RESULTS

Laser Ablation Inductively Coupled Plasma Mass Spectrometry Pyrite Analyses

Summary statistics for LA-ICP-MS analyses of pyrite from the selected deposits in the BMC are presented in Table 5. Chemical compositions of pyrite are the average of 3 or 4 spot analyses. As demonstrated in previous studies, the measured trace element contents of pyrite are extremely variable (McClenaghan et al. (2004) using EMPA; McClenaghan et al. (2009) using LA-ICP-MS). LA-ICP-MS data presented in this study show that most pyrite in the BMC is arsenian, with As contents ranging from below the lower limit of detection (BDL) to 7.3 wt% (Soltani Dehnavi et al., 2012, 2013a,b, 2014a,b,c,d). In the samples analyzed, As is the most prevalent substitution in the pyrite structure. Arsenian pyrite also contains Sb (up to 2910 ppm), Tl (up to 4110 ppm), Au (up to 73.2 ppm), Hg (up to 220

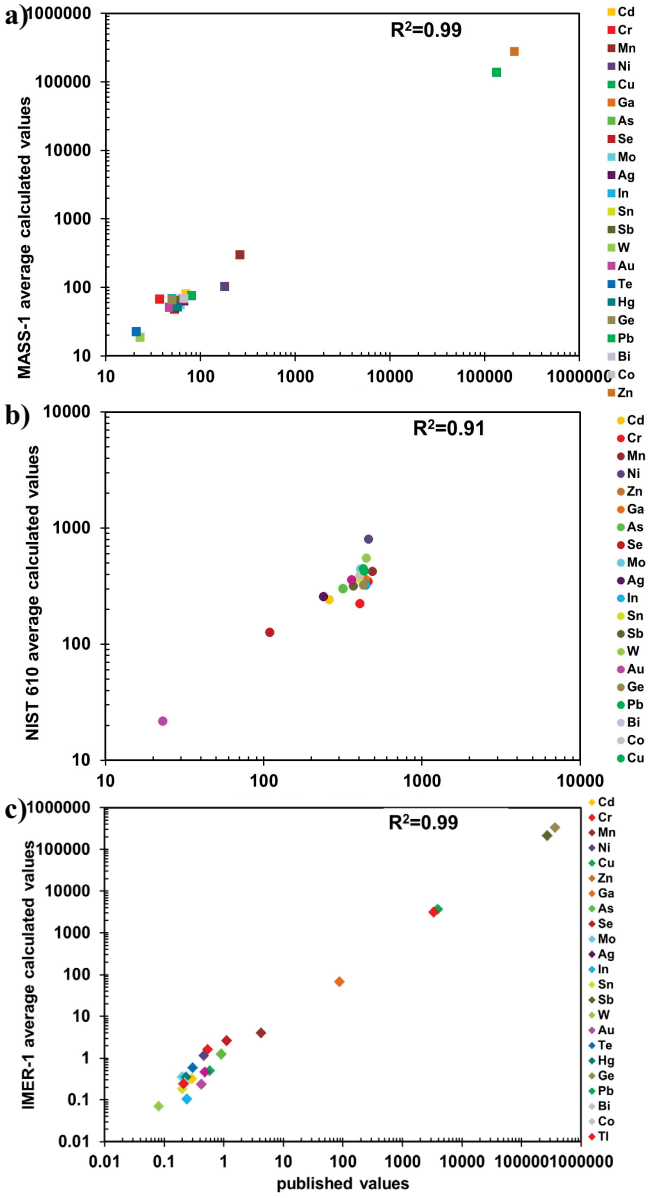

Figure 4. Binary plots comparing LA-ICP-MS results calculated by this study for elemental contents of standards MASS-1, NIST610, and IMER-1 to the published values for each standard. The strong correlation between the values is established for MASS-1 and IMER-1 and in slightly lower degree for NIST610.

ppm), In (up to 49 ppm), and Cd (up to 270 ppm) (Table 5, Fig. 6). There is a strong positive correlation between Sb and Tl, with the highest values in the Louvicourt deposit (Fig. 6a). Likewise, moderate correlations of both Sb and Tl with As show the highest values in the Louvicourt deposit (Fig. 6b,c). Antimony and Hg display a statistically poor positive correlation, with highest Hg values in the Louvicourt deposit (Fig. 6d). Indium and Cd are typically only present in low abundances (Fig. 6e). Contents of Bi exhibit positive correlation with Cu in all of the deposits except Louvicourt (Fig. 6f).

Table 4. Summary of obtained compositional variations of NIST 610, 612, and MASS-1 in this study (ppm).

	Calculated NIST 612_Si (n>150)				Calculated NIST 610_Si (n>100)				Calculated MASS-1 vs. NIST 610_Fe (n>100)			
Analyte	Min	Mean	Max	Published	Min	Mean	Max	Published	Min	Mean	Max	Suggested
Li	38.9	41.6	45.8	42	460	489	510	485	0.13	0.94	24.3	
Na	97750	100518	102750	103858	100820	102583	105090	99415	28310	36745	55300	25080
Mg	59.2	61.1	64	77	566	586	602	465	31.4	38.7	74	
Al	10959	11184	11420	11167	10560	10768	11080	10797	13.3	20.7	133	
Cl	100	172	247	131	180	359	627	438	2609	5302	13400	
K	60.3	63.7	66.3	66.3	489	506	535	486	34.6	48.2	100	
Ca	83210	84805	87700	85002	80050	82255	84760	82144	11.7	52.6	945	
Ti	35.8	38.9	45.7	44	436	493	526	434	2.04	6.8	28.2	
Cr	31	35.1	38.7	36	381	412	439	405	60.5	67.5	78.7	37
Mn	38.3	41.3	42.38	38	437	447	496	485	260	312	427	260
Fe	44.7	71.5	95.4	51	301	353	525	458				156000
Co	33.4	34.2	35.1	35	404	415	424	405	61.2	74.9	103	67
Ni	36.3	38.3	39.8	38.8	454	464	479	459	89.2	115	153	180
Cu	30.2	37.0	42.2	37	386	434	522	430	107600	153734	211600	134000
Zn	36.6	37.9	39.4	38	441	457	478	456	225500	297115	406000	207383
As	30.6	35.6	43.3	37	256	330	382	317	63	75	88	65
Rb	30.7	31.5	32.2	31.4	416	425	438	426	0.02	0.12	4.19	
Sr	71.3	76.8	79.4	78.4	509	527	578	516	0.38	0.62	11.9	
Cd	23.8	27.4	29.9	28.3	240	267	304	259	59.4	96.4	140	70
In	34.0	36.2	37.5	43	508	525	562	441	56.4	71.4	105	50
Sn	33.2	34.2	34.9	38	432	441	449	396	BDL	61.3	94.4	55
Sb	29.8	31.0	32.2	38	437	451	469	369	55.9	70.4	107	55
Cs	38.4	40.7	42.4	42	357	373	401	361	BDL	0.04	1.90	
Ba	36.6	37.7	39.0	39.7	446	459	469	435	0.64	3.05	83	
Hg	0.1	0.20	0.54		0.24	0.71	1.6		26.5	60.5	87.6	57
Tl	9.1	16.1	29.3	15.1	31	60.3	98.3	61	67.2	85.9	141	68.32
Pb	35.9	37.9	39.3	38.6	413	433	462	426	62.5	82.0	131	80
Bi	29.0	30.8	32.4	30	332	350	379	358	54.2	70.4	113	66

NOTE: BDL = below detection limit

Laser Ablation Inductively Coupled Plasma Mass Spectrometry Phyllosilicate Analyses

Summary statistics for LA-ICP-MS analyses of chlorite and white mica from representative major deposits of the BMC are presented in Table 6. McClenaghan (2011) reported that the compositions for white mica compositions in the BMC show a compositional variation between muscovite and phengite end-members. In addition, chlorite in the BMC is typically Fe-rich, although Mg-rich varieties also present (Peter et al., 2003a,b; McClenaghan, 2011). Our LA-ICP-MS data show that white mica typically contains As (below detection limit, 10100 ppm), Sb (BDL 4750 ppm), Tl (BDL 698 ppm), Hg (BDL 67 ppm), Cd (BDL 8.9 ppm), and Bi (BDL 15.7 ppm); however, Cd (BDL 83 ppm) and Bi (BDL 185 ppm) are preferentially more enriched in chlorite than in white mica (Fig. 7).

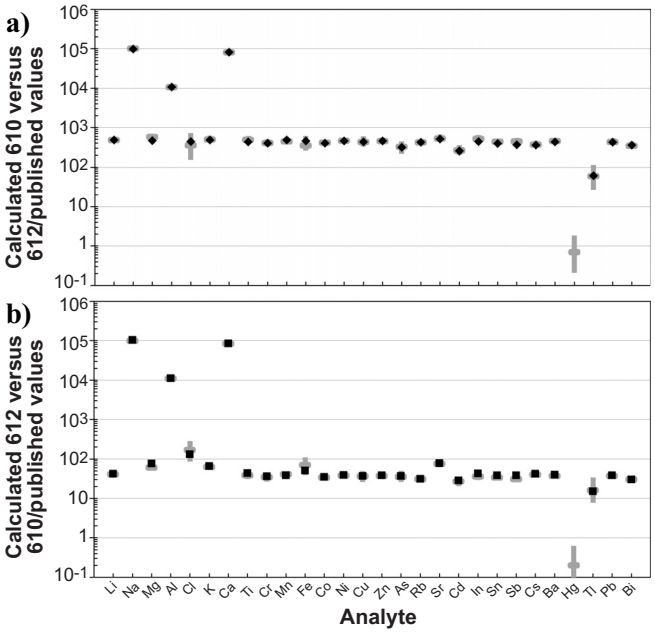

Figure 5. Assessment of the accuracy of data obtained from the calculation of standards NIST610 and NIST612, which were analyzed together with silicate samples. The average calculated values are compared to the published values for each standard. The plots show similar values for most of the elements. Internal standardization was obtained from the data published for these standards (Si). Grey bars show the range (minimum and maximum) of the elements that were examined.

DISCUSSION

Volatile Trace Element Dispersion Haloes

Volatile trace elements are potential pathfinders in geochemical prospecting for a wide variety of base- and precious-metal deposits. The characteristics of volatile trace elements that make them potential vectors is their presence in mineralizing fluids, their relatively high

Table 5. Summary of compositional variations of pyrite (LA-ICP-MS) for representative massive sulphide deposits of the Bathurst Mining Camp, New Brunswick (values in ppm).

Deposit		Drillhole	n	Fe	S	Cr	Mn	Co	Ni	Cu	Zn	Ga	Ge	As	Se	Mo	Ag	Cd	In
	MDL		792	24.65	1668	0.45	1.49	0.46	3.66	0.51	1.66	0.49	2.07	0.99	2.50	0.61	0.19	0.53	0.03
Armstrong A	Max	A-14		561000	569000	5.60	2600	750	540	5700	3600	42.1	8.90	6880	37.4	142.7	36	30.6	12.3
	Mean		54	498630	502944	1.17	206	83.5	28.3	555	186	1.57	BDL	2111	7.44	8.25	6.89	1.64	0.55
	Min			434000	446000	BDL	BDL	BDL	BDL	0.66	BDL	BDL	BDL	19.5	BDL	BDL	BDL	BDL	BDL
Brunswick No. 6	Max	B-259		657000	582000	1.56	207	1850	960	1750	50000	4.30	BDL	5690	43.9	12.8	82.0	98.0	45.3
	Mean		47	514872	491647	0.59	21.6	306	72.3	171	1461	BDL	BDL	1511	5.57	1.31	11.8	2.92	3.03
	Min			420000	382000	BDL	BDL	BDL	BDL	BDL	BDL	BDL	BDL	4.00	BDL	BDL	BDL	BDL	BDL
Caribou	Max	62-55		636000	549000	9.80	1770	915	1170	10470	243000	13.4	7	29700	710	29.8	117	260	49
	Mean		52	539135	466438	1.22	117	146	102	727	7331	1.14	BDL	1856	25.2	1.95	16.2	11.8	1.90
	Min			440000	405000	BDL	BDL	BDL	BDL	BDL	BDL	BDL	BDL	BDL	BDL	BDL	BDL	BDL	BDL
Halfmile Lake	Max	HN-119		571000	547000	19.2	4500	2620	41600	2070	8500	16.9	3.18	5800	604	9.80	50.3	21.8	14
	Mean		47	518362	481338	1.65	170	400	1485	192	392	1.00	BDL	1047	51.2	0.98	6.73	1.09	0.77
	Min			469000	431000	BDL	BDL	2.22	BDL	BDL	BDL	BDL	BDL	BDL	BDL	BDL	BDL	BDL	BDL
Restigouche	Max	CP-39		594000	540000	3.01	876	2210	1080	4950	107000	0.55	21.9	18700	720	38.2	183	135	43.9
	Mean		51	543137	465922	0.87	102	101	89.7	578	2701	BDL	2.98	1491	24.7	1.59	18.1	4.85	0.95
	Min			462000	412000	BDL	BDL	BDL	BDL	BDL	BDL	BDL	BDL	2.39	BDL	BDL	BDL	BDL	BDL
Heath Steele	Max	B-3409		602000	553000	2.20	16.5	12700	858	1900	10.2	2.32	2.70	7970	251	1.43	5.80	BDL	0.31
	Mean		29	542759	461034	0.95	1.53	858	129	116	BDL	BDL	BDL	1320	45.6	0.27	1.28	BDL	0.04
	Min			470000	400000	BDL	BDL	BDL	BDL	0.80	BDL	BDL	BDL	2.46	BDL	BDL	BDL	BDL	BDL
Canoe Landing Lake	Max	CL-94		782000	7000000	650	13840	19900	20200	564000	8000	1180	900	73000	5600	1390	1010	270	21.6
	Mean		159	572919	483824	11.8	452	792	1236	20179	351	10.7	9.50	3012	74.1	15.7	24.5	3.90	0.55
	Min			41200	318000	BDL	BDL	BDL	BDL	BDL	BDL	BDL	BDL	BDL	BDL	BDL	BDL	BDL	BDL
Key Anacon	Max	KA-93-42		719000	550000	4.9	2070	12200	5890	2750	3000	1.31	3.4	8150	293	15.2	70.0	8.20	2.90
	Mean		64	562844	457209	0.86	70.7	658	479	171	57.1	BDL	BDL	1474	32.4	0.69	4.30	BDL	0.10
	Min			447000	352000	BDL	BDL	BDL	BDL	BDL	BDL	BDL	BDL	BDL	BDL	BDL	BDL	BDL	BDL
Brunswick No. 12	Max	A1		707000	624000	7.00	2590	5740	23490	6800	26200	11.0	3.60	16200	52.3	39.7	313	57.0	19.2
	Mean		203	531756	479107	1.23	50.0	590	428	140	218	0.52	BDL	2038	5.35	1.61	11.3	0.68	0.17
	Min			403000	357000	BDL	BDL	BDL	BDL	BDL	BDL	BDL	BDL	BDL	BDL	BDL	BDL	BDL	BDL
Louvicourt	Max	LGF-6		746000	627000	2.45	2310	1300	1660	563000	4200	120	4.23	31300	26.0	94.0	2710	12.2	3.32
	Mean		86	633547	397523	0.71	117	111	144	13334	100	1.96	BDL	5497	3.30	8.26	78.9	0.77	0.13
	Min			381000	338000	BDL	BDL	BDL	BDL	BDL	BDL	BDL	BDL	BDL	BDL	BDL	BDL	BDL	BDL

NOTE: BDL = below detection limit

Table 5 continued.

Deposit		Drillhole	Sn	Sb	Te	W	Au	Hg	Tl	Pb	Bi	Fe	S	Cr	Mn	Co	Ni	Cu
	MDL		0.15	0.29	0.99	0.04	0.04	0.39	0.13	0.11	0.04	24.65	1668	0.45	1.49	0.46	3.66	0.51
Armstrong A	Max	A-14	2600	1744	2.68	13.2	0.49	24.5	217	9200	239	561000	569000	5.60	2600	750	540	5700
	Mean		58.6	145	BDL	0.78	0.11	1.65	29.7	820	36.3	498630	502944	1.17	206	83.5	28.3	555
	Min		BDL	BDL	BDL	BDL	BDL	BDL	BDL	2.29	BDL	434000	446000	BDL	BDL	BDL	BDL	0.66
Brunswick No. 6	Max	B-259	15200	1448	1.45	11.9	2.01	15.1	178	22700	319	657000	582000	1.56	207	1850	960	1750
	Mean		398	112	BDL	1.06	0.18	0.70	22.2	1695	45.2	514872	491647	0.59	21.6	306	72.3	171
	Min		BDL	BDL	BDL	BDL	BDL	BDL	BDL	BDL	BDL	420000	382000	BDL	BDL	BDL	BDL	BDL
Caribou	Max	62-55	11100	1012	10.1	6.70	7.47	17.4	280	450000	890	636000	549000	9.80	1770	915	1170	10470
	Mean		237	112	1.12	0.29	0.83	1.11	8.64	11215	109	539135	466438	1.22	117	146	102	727
	Min		BDL	BDL	BDL	BDL	BDL	BDL	BDL	0.15	BDL	440000	405000	BDL	BDL	BDL	BDL	BDL
Halfmile Lake	Max	HN-119	4800	1880	15.3	2.35	2.11	1.96	233	18600	321	571000	547000	19.2	4500	2620	41600	2070
	Mean		105	169	1.45	0.11	0.27	BDL	12.4	979	45.3	518362	481338	1.65	170	400	1485	192
	Min		BDL	BDL	BDL	BDL	BDL	BDL	BDL	0.17	BDL	469000	431000	BDL	BDL	2.22	BDL	BDL
Restigouche	Max	CP-39	137	830	22.3	10.1	9.60	2.74	250	50900	0.78	594000	540000	3.01	876	2210	1080	4950
	Mean		4.10	85.2	BDL	1.22	0.57	0.41	9.52	3301	0.14	543137	465922	0.87	102	101	89.7	578
	Min		BDL	BDL	BDL	BDL	BDL	BDL	BDL	0.10	BDL	462000	412000	BDL	BDL	BDL	BDL	BDL
Heath Steele	Max	B-3409	9.91	229	55.4	0.92	7.90	BDL	8.25	1140	108	602000	553000	2.20	16.5	12700	858	1900
	Mean		0.72	20.6	4.33	0.13	0.35	BDL	0.93	118	31.1	542759	461034	0.95	1.53	858	129	116
	Min		BDL	BDL	BDL	BDL	BDL	BDL	BDL	BDL	BDL	470000	400000	BDL	BDL	BDL	BDL	0.80
Canoe Landing Lake	Max	CL-94	2600	2473	141	25100	13.3	140	1660	84900	293	782000	7000000	650	13840	19900	20200	564000
	Mean		35.8	228	5.23	160	0.74	3.53	18.5	3376	28.5	572919	483824	11.8	452	792	1236	20179
	Min		BDL	BDL	BDL	BDL	BDL	BDL	BDL	BDL	BDL	41200	318000	BDL	BDL	BDL	BDL	BDL
Key Anacon	Max	KA-93-42	460	249	66.4	14.3	0.51	7.28	1336	39000	169	719000	550000	4.9	2070	12200	5890	2750
	Mean		9.63	24.7	2.97	0.74	0.08	BDL	25.7	1847	19.5	562844	457209	0.86	70.7	658	479	171
	Min		BDL	BDL	BDL	BDL	BDL	BDL	BDL	BDL	BDL	447000	352000	BDL	BDL	BDL	BDL	BDL
Brunswick No. 12	Max	A1	88.0	2910	96.4	3.02	5.20	4.47	208	6900	790	707000	624000	7.00	2590	5740	23490	6800
	Mean		1.82	117	2.54	0.25	0.34	BDL	7.10	403	49.7	531756	479107	1.23	50.0	590	428	140
	Min		BDL	BDL	BDL	BDL	BDL	BDL	BDL	BDL	BDL	403000	357000	BDL	BDL	BDL	BDL	BDL
Louvicourt	Max	LGF-6	7.60	2800	10.1	9.90	73.2	220	4110	48000	87.0	746000	627000	2.45	2310	1300	1660	563000
	Mean		0.27	359	1.02	0.40	1.86	8.91	197	3682	4.64	633547	397523	0.71	117	111	144	13334
	Min		BDL	BDL	BDL	BDL	BDL	BDL	BDL	0.38	0.04	381000	338000	BDL	BDL	BDL	BDL	BDL

NOTE: BDL = below detection limit

Table 5 continued.

Deposit		Drillhole	Zn	Ga	Ge	As	Se	Mo	Ag	Cd	In	Sn	Sb	Te	W	Au	Hg	Tl	Pb	Bi
	MDL		1.66	0.49	2.07	0.99	2.50	0.61	0.19	0.53	0.03	0.15	0.29	0.99	0.04	0.04	0.39	0.13	0.11	0.04
Armstrong A	Max	A-14	3600	42.1	8.90	6880	37.4	142.7	36	30.6	12.3	2600	1744	2.68	13.2	0.49	24.5	217	9200	239
	Mean		186	1.57	BDL	2111	7.44	8.25	6.89	1.64	0.55	58.6	145	BDL	0.78	0.11	1.65	29.7	820	36.3
	Min		BDL	BDL	BDL	19.5	BDL	BDL	BDL	BDL	BDL	BDL	BDL	BDL	BDL	BDL	BDL	BDL	2.29	BDL
Brunswick No. 6	Max	B-259	50000	4.30	BDL	5690	43.9	12.8	82.0	98.0	45.3	15200	1448	1.45	11.9	2.01	15.1	178	22700	319
	Mean		1461	BDL	BDL	1511	5.57	1.31	11.8	2.92	3.03	398	112	BDL	1.06	0.18	0.70	22.2	1695	45.2
	Min		BDL	BDL	BDL	4.00	BDL	BDL	BDL	BDL	BDL	BDL	BDL	BDL	BDL	BDL	BDL	BDL	BDL	BDL
Caribou	Max	62-55	243000	13.4	7	29700	710	29.8	117	260	49	11100	1012	10.1	6.70	7.47	17.4	280	450000	890
	Mean		7331	1.14	BDL	1856	25.2	1.95	16.2	11.8	1.90	237	112	1.12	0.29	0.83	1.11	8.64	11215	109
	Min		BDL	BDL	BDL	BDL	BDL	BDL	BDL	BDL	BDL	BDL	BDL	BDL	BDL	BDL	BDL	BDL	0.15	BDL
Halfmile Lake	Max	HN-119	8500	16.9	3.18	5800	604	9.80	50.3	21.8	14	4800	1880	15.3	2.35	2.11	1.96	233	18600	321
	Mean		392	1.00	BDL	1047	51.2	0.98	6.73	1.09	0.77	105	169	1.45	0.11	0.27	BDL	12.4	979	45.3
	Min		BDL	BDL	BDL	BDL	BDL	BDL	BDL	BDL	BDL	BDL	BDL	BDL	BDL	BDL	BDL	BDL	0.17	BDL
Restigouche	Max	CP-39	107000	0.55	21.9	18700	720	38.2	183	135	43.9	137	830	22.3	10.1	9.60	2.74	250	50900	0.78
	Mean		2701	BDL	2.98	1491	24.7	1.59	18.1	4.85	0.95	4.10	85.2	BDL	1.22	0.57	0.41	9.52	3301	0.14
	Min		BDL	BDL	BDL	2.39	BDL	BDL	BDL	BDL	BDL	BDL	BDL	BDL	BDL	BDL	BDL	BDL	0.10	BDL
Heath Steele	Max	B-3409	10.2	2.32	2.70	7970	251	1.43	5.80	BDL	0.31	9.91	229	55.4	0.92	7.90	BDL	8.25	1140	108
	Mean		BDL	BDL	BDL	1320	45.6	0.27	1.28	BDL	0.04	0.72	20.6	4.33	0.13	0.35	BDL	0.93	118	31.1
	Min		BDL	BDL	BDL	2.46	BDL	BDL	BDL	BDL	BDL	BDL	BDL	BDL	BDL	BDL	BDL	BDL	BDL	BDL
Canoe Landing Lake	Max	CL-94	8000	1180	900	73000	5600	1390	1010	270	21.6	2600	2473	141	25100	13.3	140	1660	84900	293
	Mean		351	10.7	9.50	3012	74.1	15.7	24.5	3.90	0.55	35.8	228	5.23	160	0.74	3.53	18.5	3376	28.5
	Min		BDL	BDL	BDL	BDL	BDL	BDL	BDL	BDL	BDL	BDL	BDL	BDL	BDL	BDL	BDL	BDL	BDL	BDL
Key Anacon	Max	KA-93-42	3000	1.31	3.4	8150	293	15.2	70.0	8.20	2.90	460	249	66.4	14.3	0.51	7.28	1336	39000	169
	Mean		57.1	BDL	BDL	1474	32.4	0.69	4.30	BDL	0.10	9.63	24.7	2.97	0.74	0.08	BDL	25.7	1847	19.5
	Min		BDL	BDL	BDL	BDL	BDL	BDL	BDL	BDL	BDL	BDL	BDL	BDL	BDL	BDL	BDL	BDL	BDL	BDL
Brunswick No. 12	Max	A1	26200	11.0	3.60	16200	52.3	39.7	313	57.0	19.2	88.0	2910	96.4	3.02	5.20	4.47	208	6900	790
	Mean		218	0.52	BDL	2038	5.35	1.61	11.3	0.68	0.17	1.82	117	2.54	0.25	0.34	BDL	7.10	403	49.7
	Min		BDL	BDL	BDL	BDL	BDL	BDL	BDL	BDL	BDL	BDL	BDL	BDL	BDL	BDL	BDL	BDL	BDL	BDL
Louvicourt	Max	LGF-6	4200	120	4.23	31300	26.0	94.0	2710	12.2	3.32	7.60	2800	10.1	9.90	73.2	220	4110	48000	87.0
	Mean		100	1.96	BDL	5497	3.30	8.26	78.9	0.77	0.13	0.27	359	1.02	0.40	1.86	8.91	197	3682	4.64
	Min		BDL	BDL	BDL	BDL	BDL	BDL	BDL	BDL	BDL	BDL	BDL	BDL	BDL	BDL	BDL	BDL	0.38	0.04

NOTE: BDL = below detection limit

Table 6. Summary of compositional variations of phyllosilicate minerals (LA-ICP-MS) for representative massive sulphide deposits of the Bathurst Mining Camp, New Brunswick (values in ppm).

Deposit	Halfmile	Drillhole	Mineral	n	Li	Na	Mg	Al	Cl	K	Ca	Ti	Cr	Mn	Fe	Co	Ni	Cu
	MDL			512	1.83	6.39	0.40	1.35	64.6	4.76	59.9	2.23	2.84	1.79	10.6	0.12	0.76	0.24
Halfmile Lake	Max	HN-119	White mica		110.30	57560	175100	218600	2090	104630	34610	25400	297	13484	389000	156	59	33
	Mean			81	21.61	3213	23215	147096	260	82253	1265	2350	67.3	910	56693	7.50	9.43	3.00
	Min				2.13	28.7	3960	16500	BDL	43	BDL	169	BDL	33.7	1278	0.15	BDL	BDL
Halfmile Lake	Max	HN-119	Chlorite		65.40	29580	87010	121200	1190	48170	8470	27400	431	6810	315000	96	169	88
	Mean			127	23.50	1144	53087	93197	132	7333	364	696	37.8	2987	154575	13.1	18.0	2.10
	Min				BDL	BDL	497	26200	BDL	BDL	BDL	38.1	BDL	7.2	840	BDL	BDL	BDL
Heath Steele	Max	B-3409	White mica		93.80	19040	48800	204400	3300	108760	23400	15800	250	4800	244000	65	169	23600
	Mean			117	29.15	2631	15986	150039	197	88503	598	2291	39.1	686	40559	4.80	7.18	205
	Min				4.20	126	4718	22900	BDL	7000	BDL	137	BDL	64.6	11330	0.65	BDL	BDL
Heath Steele	Max	B-3409	Chlorite		131.20	19900	92500	122300	3700	54700	145000	33200	297	20930	289800	188	222	10.4
	Mean			91	26.55	1797	34812	76278	271	8530	5426	1048	23.3	3546	128908	18.2	16.5	0.93
	Min				BDL	BDL	1412	2020	BDL	4.7	BDL	3.9	BDL	8.80	820	0.16	BDL	BDL
Louvicourt	Max	LGF-6	White mica		65.10	1232	37080	175800	7300	108160	52800	12900	353	24300	306000	142	124.1	13530
	Mean			47	42.80	818	18255	147907	761	94919	1820	2985	51.1	1265	47741	10.9	27.3	351
	Min				18.50	293	8360	59400	BDL	37200	BDL	65.8	3	190	7390	BDL	BDL	BDL
Louvicourt	Max	LGF-6	Chlorite		85.80	391	105800	105700	1700	52750	72800	4500	953	21200	372000	150	498	208
	Mean			31	42.91	80	61350	86978	284	7248	3354	868	40.3	4777	157764	61.1	210	7.59
	Min				10.50	BDL	8048	28600	11.1	11.2	15.9	70	0.53	151	19640	0.14	7.09	BDL

Table 6 continued.

Deposit	Halfmile	Drillhole	Mineral	Zn	As	Se	Rb	Sr	Cd	In	Sn	Sb	Te	Cs	Ba	Hg	Tl	Pb	Bi
	MDL			0.56	3.36	2.50	0.17	0.01	0.13	0.02	0.07	0.17	0.69	0.07	0.12	0.13	0.02	0.03	0.04
Halfmile Lake	Max	HN-119	White mica	1466	700	41.3	587	63.1	0.31	3.1	253	5.4	0.96	16.1	2337	2.89	43.5	129	15.7
	Mean			93.3	26.1	BDL	353	17.2	BDL	0.45	29.4	1.30	BDL	4.82	992	0.87	3.79	4.54	0.46
	Min			2.71	BDL	BDL	0.22	0.75	BDL	0.15	0.54	BDL	BDL	0.11	0.22	BDL	BDL	0.43	BDL
Halfmile Lake	Max	HN-119	Chlorite	83500	1110	109	222	45.7	83.2	42.2	104	4.3	0.97	15.5	741	3.84	13.23	39000	10.1
	Mean			2036	17.7	BDL	31.2	4.39	1.79	1.16	3.68	0.32	0.26	1.07	81.4	0.51	0.58	315	0.29
	Min			2.87	BDL	BDL	BDL	0.07	BDL	BDL	BDL	BDL	BDL	BDL	BDL	0.06	BDL	BDL	BDL
Heath Steele	Max	B-3409	White mica	402	23	57	664	185	0.84	21.6	359	7.3	0.96	22.4	10130	1.93	15.0	28.2	10.8
	Mean			93.5	5.96	BDL	427	27.4	BDL	0.64	24.8	1.33	BDL	6.44	1539	0.82	4.17	4.46	0.15
	Min			8.81	BDL	BDL	32.5	2.21	BDL	0.12	0.77	BDL	BDL	0.36	74.3	BDL	0.54	0.35	BDL
Heath Steele	Max	B-3409	Chlorite	1161	192	8.8	229	423	9.5	1.1	22.9	51.1	3.60	10.1	1728	1.13	5.21	285000	185
	Mean			317	14.0	BDL	34.8	15.8	0.19	0.19	2.42	2.63	BDL	1.03	162	0.41	0.60	3374	2.90
	Min			1.47	BDL	BDL	BDL	0.07	BDL	BDL	BDL	BDL	BDL	BDL	BDL	BDL	BDL	BDL	BDL
Louvicourt	Max	LGF-6	White mica	2332	10100	7.4	465	2795	8.19	511	981	4750	1.5	7.36	250200	67.1	698	4680	1.32
	Mean			453	250	2.70	367	120	0.43	30.7	75.4	117	BDL	4.53	26315	4.43	186	478	0.15
	Min			71.3	BDL	BDL	143	3.03	BDL	0.05	2.59	1.17	BDL	1.86	5650	0.36	49.7	0.87	BDL
Louvicourt	Max	LGF-6	Chlorite	6400	17.2	2.81	189	1210	0.85	384	983	2.06	0.50	2.41	115000	14.1	50.1	9900	1.88
	Mean			2046	7.32	BDL	26.6	153	0.12	51.9	99.6	0.75	0.27	0.49	12756	1.91	9.41	418	0.09
	Min			99.9	BDL	BDL	BDL	0.33	BDL	0.02	BDL	BDL	BDL	BDL	2.27	0.02	0.05	0.12	BDL

NOTE: BDL = below detection limit

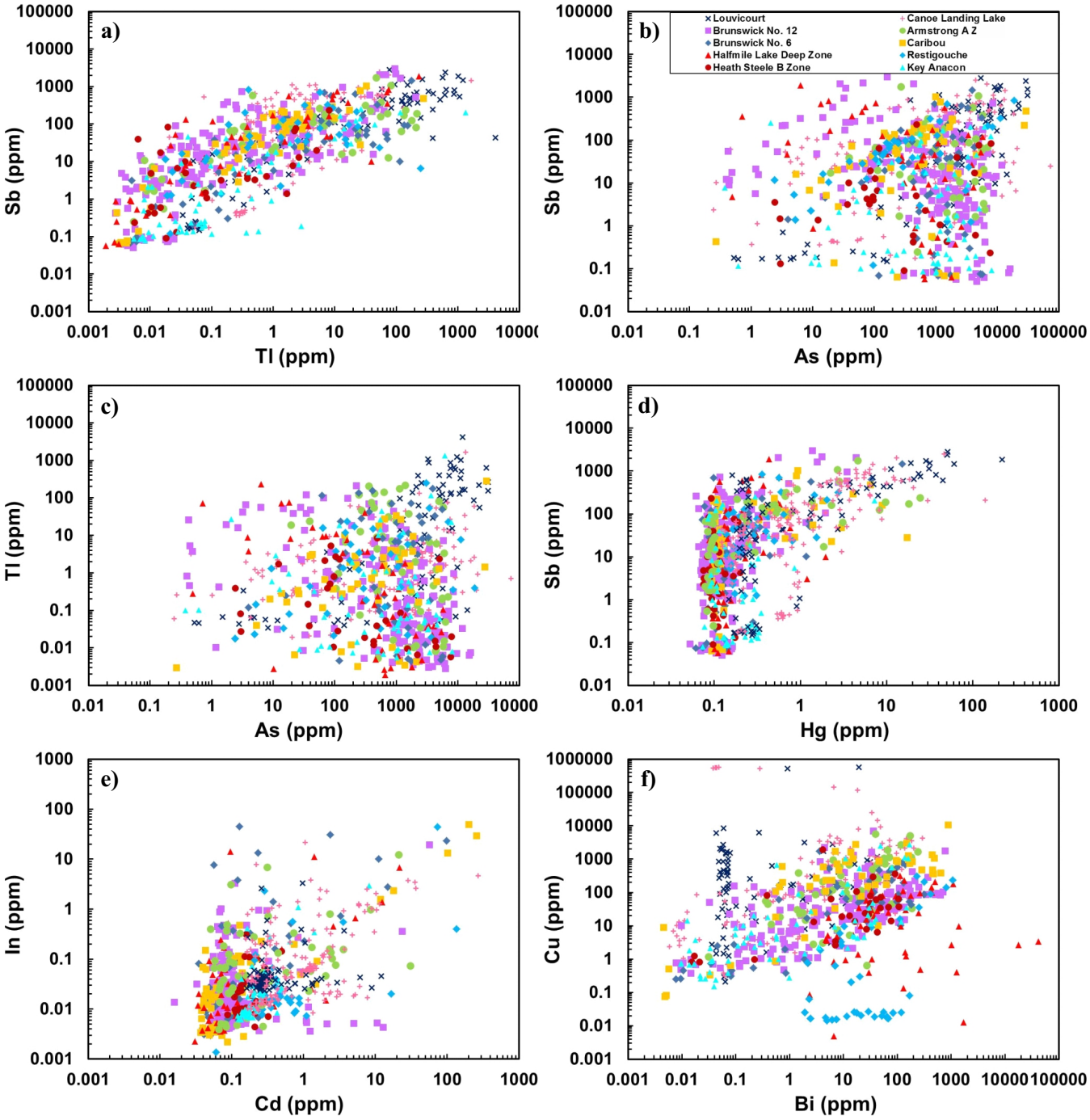

Figure 6. Binary plots of LA-ICP-MS analyses for selected volatile trace elements in pyrite from representative massive sulphide deposits of the Bathurst Mining Camp.

vapour pressure characteristics, and their role as transporting agents of metals during the mineralizing process (Ryall, 1981, and references therein; Carr et al., 1986). The volatile trace elements whose behaviour has previously been systematically and comprehensively studied in a VMS environment are Hg, Tl, and Sb (Boldy, 1963, 1979; Ryall, 1981 and references therein; Carr et al., 1986; Lentz and Goodfellow, 1993; Lentz et al., 1997; Large et al., 2001 and references therein).

A distinct primary Hg dispersion halo was documented in the hanging-wall rocks of the Norbec deposit, Noranda district, Quebec, and was considered to be a prospective exploration vector toward deeply buried and blind sulphide deposits (Boldy, 1963, 1979). Lentz and Goodfellow (1993), who studied core from the discovery drillhole (A1) at the Brunswick No. 12 deposit in the BMC, found that the distribution of hydrothermal elements displayed distinctive enrichments for Hg, Sb, and to lesser extent Tl, in the hanging wall of the deposit. Lentz et al. (1997) studied

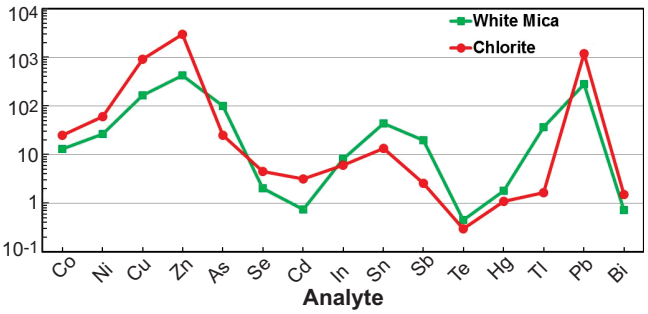

Figure 7. Comparision of average element values of chlorite and white mica obtained by LA-ICP-MS throughout the BMC, showing the relative distribution of volatile trace elements in these minerals.

whole-rock data for drillhole HSB 3409 from the Heath Steele B Zone and found increasing trends of some volatile elements, such as Hg, As, and Sb toward the ore horizon. Large et al. (2001) examined the distributions of Tl and Sb in the host-rock sequence to the Rosebery VMS deposit, Australia, and reported clearly defined, well developed, and widespread halo around the ore lenses.

In the present study, the composition of pyrite, chlorite, and white mica were examined from drillholes throughout selected deposits to identify the key residence sites of volatile trace elements. Though disseminated and vein sulphides are typically only prevalent proximal to mineralization in the BMC (Lentz et al., 1997), pyrite, which is the most widespread disseminated sulphide mineral in the footwall and hanging-wall sequences of VMS deposits can occur far (hundreds of metres) from massive sulphide mineralization (Corbett, 2001). In addition, pyrite compositions can be easily determined using LA-ICP-MS analyses and data reduction using the stoichiometric value of Fe, which can then be used as an internal standard to obtain reliable data. Finally, pyrite can contain significant contents of volatile trace elements, allowing it to be used as a potential volatile element vectoring mineral.

Chlorite and white mica are the most abundant phyllosilicate VMS-related hydrothermal alteration minerals in the BMC. Chlorite commonly occurs together with the massive sulphides (also with disseminated to semi-massive sulphides) and exhalative sedimentary rocks along mineralized horizons. White mica is ubiquitous in quartzo-feldspathic volcaniclastic rocks, siliciclastic, and exhalative sedimentary rocks. Moreover, variations in the chemical composition of chlorite and white mica can serve as a tool in discovering mineralization at depth. To demonstrate the applicability of these proposed vectoring minerals, integrated LA-ICP-MS volatile trace element data for pyrite and phyllosilicates have been plotted on drillhole stratigraphic logs (Figs. 8, 9).

Volatile Element Vectoring using Pyrite

The chemical variability of pyrite in alteration zones (massive sulphides and epithermal gold veins) from hanging wall to footwall has been shown to be an indicator of mineralization processes that can potentially be used in exploration (Roberts, 1982; Baker et al., 2006). Rogers et al. (2014) successfully used the trace element compositions of pyrite to identify high-temperature, VMS-related hydrothermal up-flow zones in the vicinity of the Hébécourt VMS prospect, Abitibi greenstone belt.

Figure 8 presents stratigraphic logs of pyrite volatile element profiles for selected deposits in the BMC that were determined in the current study. The abundance of pyrite systematically increases towards the ore horizon of the studied deposits in both the hanging wall and footwall. Pyrite in the altered footwall units typically displays systematically increasing volatile trace elements with decreasing distance to the ore horizon, particularly in the Restigouche (up to 150 m), Canoe Landing Lake (about 100 m), Armstrong (about 30 m), and Heath Steele B Zone (over 150 m) deposits. However, in the hanging-wall alteration zones, there is no consistent trend in the volatile element contents of pyrite. The Brunswick No. 12, Canoe Landing Lake, Restigouche, and Key Anacon deposits show that pyrite in the upper portions of the hanging wall has distinct As enrichment together with some other volatile trace elements, such as Sb, Tl, and Bi (Fig. 8). Therefore, systematic variations in the volatile trace element compositions of pyrite from alteration zones can serve as a potential vector to mineralization in the BMC. Below is a summary of pyrite volatile trace element systematics for the different deposits that were examined.

Restigouche Deposit – CP-39

The Restigouche deposit is hosted within feldspar crystal-rich and crystal-poor sequences of the Mount Brittain Formation. The footwall to the Restigouche deposit consists of silicified and chloritic, aphyric to sparsely feldspar-phyric rhyolite flows and hyaloclastite. The hanging wall comprises hyalotuff, chert, and feldspar crystal lithic tuff containing feldspar-crystal lithic tuff interlayered with thin beds of rhyolite tuff. Pyrite is the only sulphide mineral present in the altered felsic rocks of Restigouche deposit. Volatile trace elements are enriched in pyrite in the upper portion of the hanging wall and decrease in abundance toward the bedded sulphide horizon. Pyrite from the footwall has systematically increasing In, Cd, Hg, Sb, Bi, and Tl contents (up to 150 m) toward the ore horizon, and systematically decreasing As content (Fig. 8a).

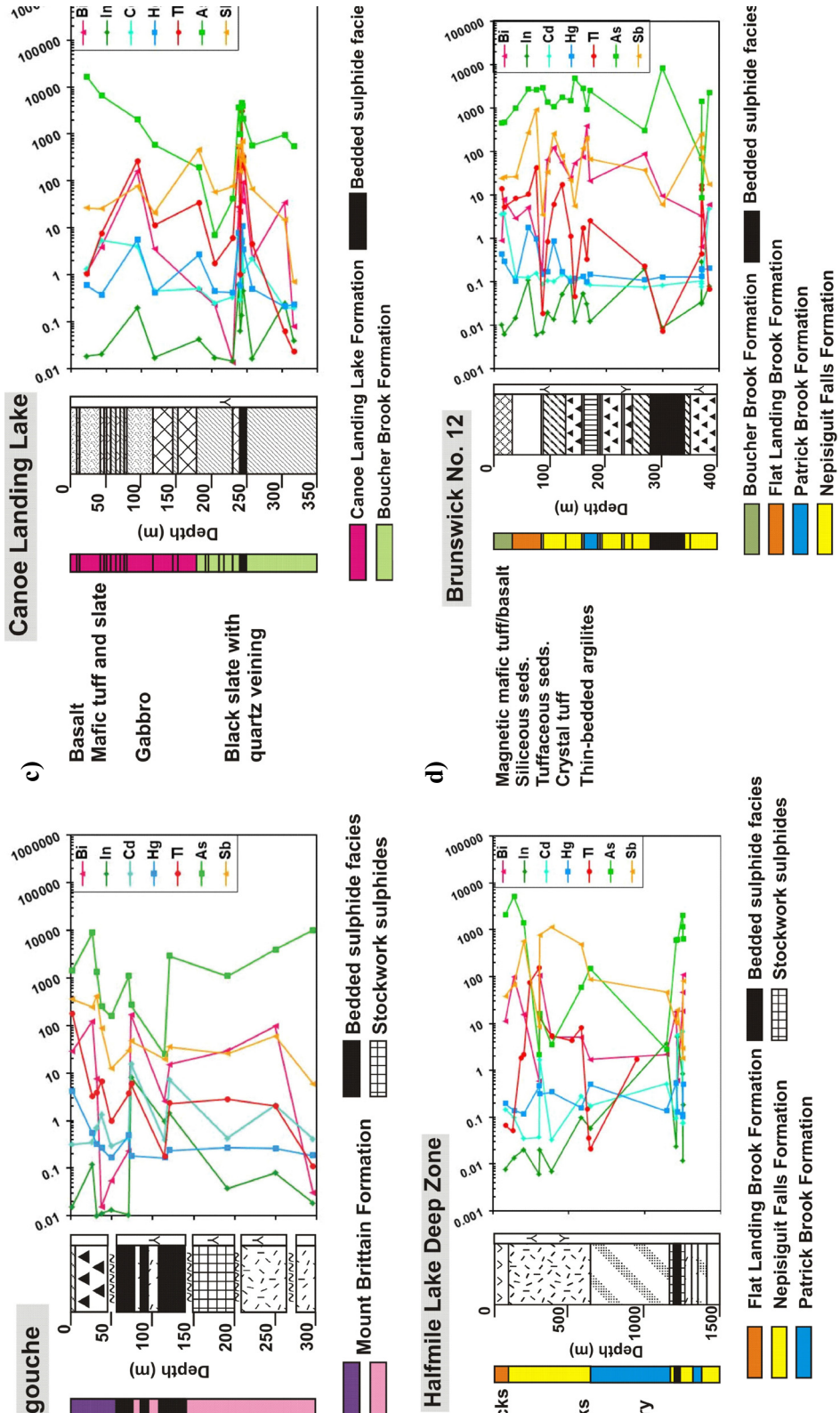

Figure 8. LA-ICP-MS geochemical data profiles illustrating volatile trace elements of pyrite plotted on the stratigraphic profiles of **a)** Restigouche deposit (CP-39); **b)** Halfmile Lake Deep Zone deposit (HN-119); **c)** Canoe Landing Lake deposit (CL-94-2); **d)** Brunswick No. 12 deposit (A-1).

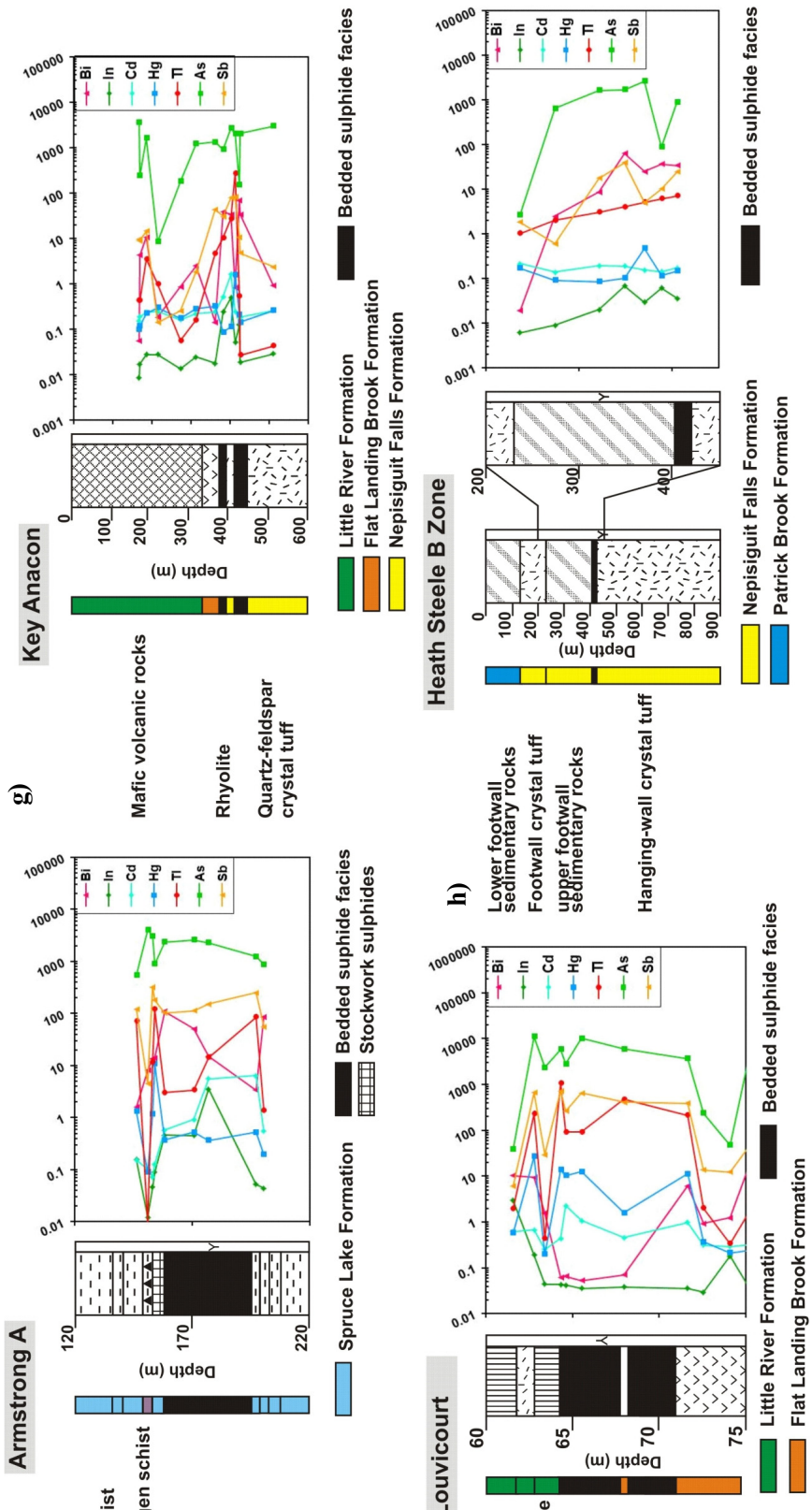

Figure 8 continued. LA-ICP-MS geochemical data profiles illustrating volatile trace elements of pyrite plotted on the stratigraphic profiles of **e)** Armstrong A Zone (A-14); **f)** Louvicourt deposit (LGF-6); **g)** Key Anacon deposit (93-42); and **h)** Heath Steele B Zone (HSB 3409).

Halfmile Lake Deep Zone – HN-119

The Halfmile Lake Deep zone is hosted within quartz-feldspar crystal tuff and volcaniclastic rocks of the Nepisiguit Falls Formation and is overlain by the sedimentary rocks of the Patrick Brook Formation. The Nepisiguit Falls Formation is within the upward-facing limb of the Halfmile Lake anticline. The Patrick Brook Formation lies below the Nepisiguit Falls Formation, and has been hydrothermally altered to a high degree (Mireku and Stanley, 2007; Walker and McCutcheon, 2010). Drillhole HN-119 of the Halfmile Lake Deep Zone contains over 1200 m of disseminated pyrite within the structural hanging wall of the deposit. The volatile trace elements of pyrite are variably enriched in the hanging-wall crystal tuff and volcaniclastic rocks of the Nepisiguit Falls Formation (Fig. 8b).

Canoe Landing Lake – CL-94-2

The deposit is hosted by thinly bedded slate, greywacke, phyllite, hyaloclastite, epiclastic rocks and pillowed flows of the Canoe Landing Lake Formation. This package is unconformably overlain by slate, intraformational conglomerate (mélange or olistostrome), and mafic volcanic rocks of the Boucher Brook Formation. Mafic tuff and basalt of the hanging wall in drillhole CL-94-2 contain disseminated pyrite; black to grey-green slate contains pyrite as nodules and laminations. Pyrite in the hanging wall of the deposit is As-rich over an interval of 150 m, particularly within mafic tuff and basalt; As contents significantly decrease in the slate with decreasing distance toward the ore horizon. Thallium and Sb also display a subtle trend of increasing abundances with decreasing distance to the ore horizon (Fig. 8c).

Brunswick No. 12 – A-1

The Brunswick horizon occurs near the top of the Nepisiguit Falls formation within the Tetagouche Group. Rocks hosting the Brunswick No. 12 deposit have been divided into four formations. From oldest to youngest, these are the Patrick Brook, Nepisiguit Falls, Flat Landing Brook, and Little River formations. Pyrite in the hanging-wall rocks of drillhole 12-A1 are enriched in As and Sb, and to a lesser extent, Tl and Hg; pyrite of the footwall sequence does not contain significant abundances of volatile elements (Fig. 8d).

Armstrong A – A-14

The Armstrong A deposit is hosted within chloritic to sericitic quartz-feldspar augen schist and phyllite of the Spruce Lake Formation. Two samples of host rock from the hanging wall show trends of increasing volatile trace element contents in pyrite with decreasing distance to the ore horizon. Pyrite from the stockwork of the deposit displays enrichment of volatile elements, especially As and Sb (Fig. 8e).

Louvicourt – LGF-6

The Louvicourt deposit is hosted within rhyolitic tuff, argillite, and basalt of the Flat Landing Brook Formation. It has been folded into anticlinal and synformal structures plunging 80° to the west, and are in thrust contact with basalt of the Little River Formation (Rose and Johnson, 1990). Pyrite in altered rhyolite of the footwall in drillhole LGF-6 from the Louvicourt deposit displays trends of increasing abundances for almost all of the volatile trace elements with decreasing distance toward the ore horizon. Pyrite in hanging-wall samples shows trends of increasing As, Sb, Tl, and Hg, whereas Bi and In decrease with decreasing distance to the ore horizon (Fig. 8f).

Key Anacon – KA 93-42

Key Anacon is hosted by felsic and mafic volcanic rocks and related sedimentary rocks of the Tetagouche Group. The volatile trace element contents of pyrite in the upper portion of the mafic volcanic rocks of the hanging wall are enriched, and show trends of increasing contents with decreasing distance towards the ore horizon (Fig. 8g).

Heath Steele B Zone – HSB 3409

The Heath Steele B zone is hosted in crystal-rich felsic volcaniclastic rocks and associated tuffaceous sedimentary rocks of the Nepisiguit Falls Formation. Pyrite occurs only in the upper footwall sedimentary rocks. Volatile trace elements increase with decreasing distance towards the ore horizon (Fig. 8h).

Volatile Element Vectoring using Phyllosilicate Minerals

The chemical compositions of phyllosilicate minerals are commonly used to vector toward VMS mineralization (i.e. proximal versus distal haloes) (Yang et al., 2011). LA-ICP-MS data for chlorite and muscovitic to phengitic white mica plotted on stratigraphic logs demonstrate that volatile trace element contents in the Halfmile Lake (over 1200 m in the hanging wall), Heath Steele B Zone (over 400 m in the hanging wall and footwall), and Louvicourt (~5 m in both the hanging wall and footwall) deposits increase in both the hanging-wall and footwall units with decreasing distance to the ore horizon (Fig. 9). The increase in volatile trace element contents towards the upper stratigraphic sections of the drillholes shows that the volatile element contents of phyllosilicate minerals can be used to vector toward mineralization within the VMS systems of the BMC. Below is a summary of phyllosilicate volatile trace element systematics for the deposits that have been examined to date.

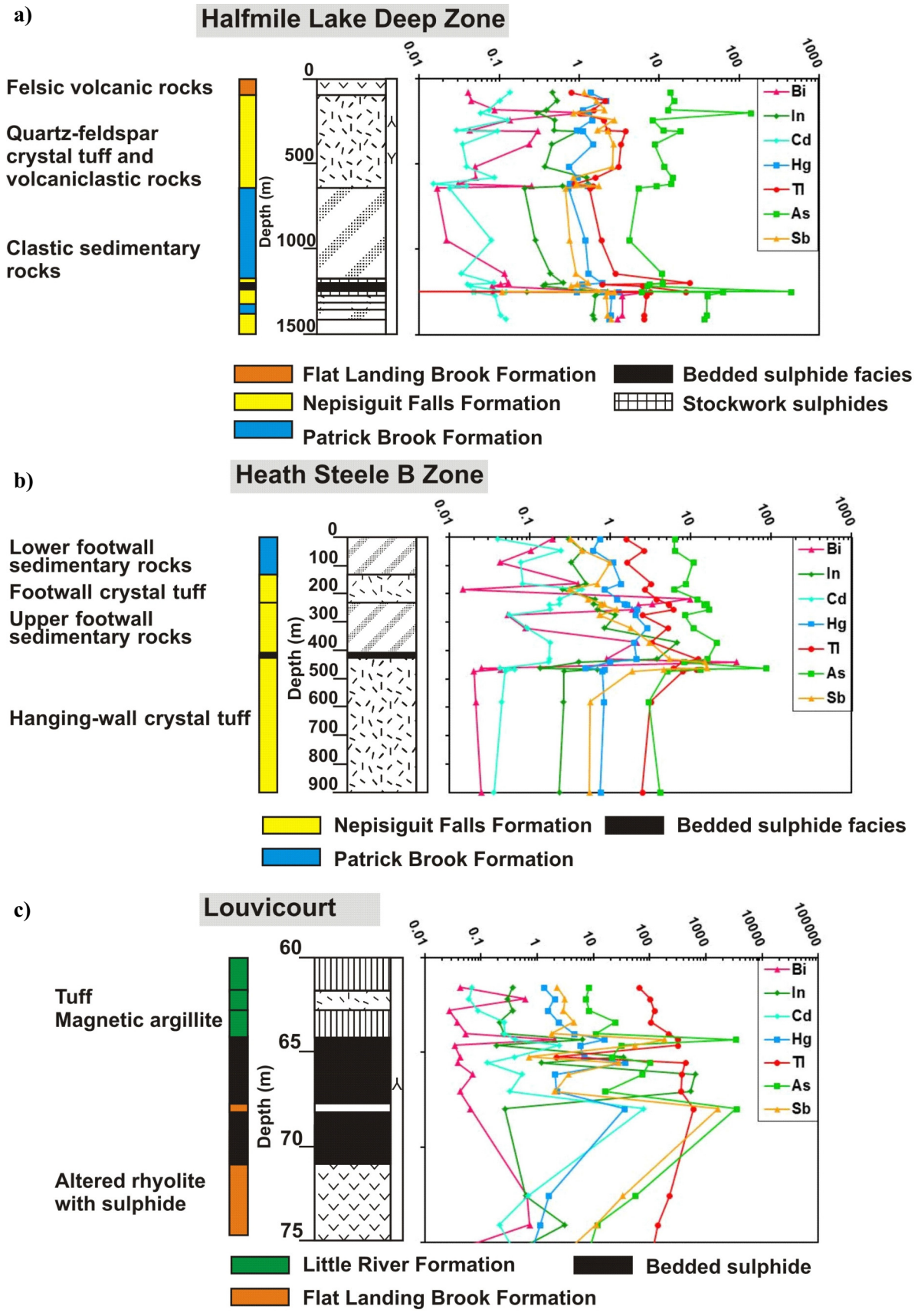

Figure 9. LA-ICP-MS geochemical data profiles illustrating volatile trace element contents of chlorite and white mica plotted on the stratigraphic profiles of **a)** Halfmile Lake Deep Zone (HN-119); **b)** Heath Steele B Zone (HSB 3409); and **c)** Louvicourt deposit (LGF-6) deposits.

Halfmile Lake Deep Zone – HN-119

Drillhole HN-119 shows higher abundances of volatile trace elements in chlorite and white mica in the crystal tuff and volcaniclastic rocks of the Nepisiguit Falls Formation than the clastic sedimentary rocks of the Patrick Brook Formation. The volatile trace elements subtly increase with decreasing distance toward the ore horizon (Fig. 9a).

Heath Steele B Zone – HSB 3409

The proportion of the K-mica and Fe-chlorite increases in the stratigraphic footwall rocks with decreasing distance to the ore horizon. This is coincident with distinctly increasing trends of volatile trace elements, in particular As, Tl, Hg, and In. (Fig. 9b).

Louvicourt – LGF-6

Chlorite and white mica within the tuffaceous argillite and chloritic iron formation in the hanging wall of the deposit have higher contents of Tl and to a lesser extent As and Sb, which systematically increase with decreasing distance towards the ore horizon. Concomitantly, the abundances of phyllosilicate minerals in the altered rhyolite in the footwall also increase with decreasing distance toward the ore horizon (Fig. 9c).

IMPLICATIONS FOR EXPLORATION

The methodology presented herein is shown to be effective in the BMC, but may also be applicable to polymetallic VMS environments elsewhere. The use of pyrite, chlorite, and white mica volatile element contents to vector toward VMS mineralization could be used as a complementary technique to field-based and other conventional exploration vectoring techniques.

FUTURE WORK

The promising results from this initial work on chlorite and white mica from a limited number of deposits will be expanded to include other deposits in the BMC. Particular focus will be placed on white mica from hydrothermal alteration zones. This will allow us to determine whether white mica volatile element compositions can serve as an indicator of proximal VMS-related hydrothermal activity, and if the volatile element data can be used to vector toward concealed mineralization.

ACKNOWLEDGEMENTS

This project is supported by funding from the Earth Science Sector, Natural Resources Canada Targeted Geoscience Initiative 4 program. We also appreciate colleagues at the Geological Survey of Canada, particularly Jan Peter (VMS Ore System Science Leader) and the New Brunswick Department of Energy and Mines in Bathurst, especially Jim Walker and Sean McClenaghan, for assistance in locating legacy datasets and samples. Allen Pring and Benjamin Wade (University of Adelaide, Australia) provided the sulphide standard (IMER-1) that was used, and Douglas Hall assisted with the micro-analytical analysis at UNB. We thank Jim Walker, Patrick Mercier-Langevin, and Jan Peter for reviews and Jan Peter for technical editing.

REFERENCES

Baker, T., Mustard, R., Brown, V., Pearson, N., Stanley, C.R., Radford, N.W., and Butler, I., 2006. Textural and chemical zonation of pyrite at Pajingo: a potential vector to epithermal gold veins; Geochemistry Exploration, Environment, Analysis, v. 6, p. 283–293.

Boldy, J., 1963. Mercury dispersion haloes as exploration targets; Falconbridge Ltd. internal report.

Boldy, J., 1979. Exploration discoveries, Noranda district, Quebec (Case History of a Mining Camp); Geological Survey of Canada, Economic Geology Report 31, p. 593– 603.

Carr, G.R., Wilmshurst, J.R., and Ryall, W.R., 1986. Evaluation of mercury pathfinder techniques: base metal and uranium deposits; Journal of Geochemical Exploration, v. 26, p. 1–117.

Chen, T.T., 1978. Colloform and framboidal pyrite from the Caribou deposit, New Brunswick; Canadian Mineralogist, v. 16, p. 9–15.

Corbett, K.D., 2001. New mapping and interpretations of the Mount Lyell mining district, Tasmania — a large hybrid Cu-Au system with an exhalative Pb-Zn top; Economic Geology, v. 96, p. 1089–1122.

Ding, L., Yang, G., Xia, F., Lenehan, C.E., Gujie Qian, G., McFadden, A., Brugger, J., Zhang, X., Chen, G., and Pring, A., 2011. A LA-ICP-MS sulphide calibration standard based on a chalcogenide glass; Mineralogical Magazine, v. 75, p. 279–287.

Goodfellow, W.D., 1975. Major and minor element haloes in volcanic rocks at Brunswick No. 12 sulphide deposit, N.B., Canada, *In:* Geochemical Exploration 1974, (ed.) I.L Elliot and W.K. Fletcher; Elsevier, Amsterdam, p. 279–295.

Goodfellow, W.D. and McCutcheon, S.R., 2003. Geologic and genetic attributes of volcanic sediment-hosted massive sulfide deposits of the Bathurst Mining Camp, northern New Brunswick–a synthesis, *In:* Massive sulfide deposits of the Bathurst mining camp, New Brunswick, and northern Maine, (ed.) W.D. Goodfellow, S.R McCutcheon, and J.M. Peter; Society of Economic Geologists, Economic Geology Monograph 11, p. 245–302.

Jambor, J.L., 1979, Mineralogical evolution of proximal distal features in New Brunswick massive sulphide deposits; Canadian Mineralogist, v. 17, p. 79–87.

Jambor, J.L., 1981, Mineralogy of Caribou massive sulphide deposit, Bathurst area, New Brunswick, Canada; Natural Resources Canada, CANMET Report 81-8E, 65 p.

Large, R.R., Allen, R.L., Blake, M.D., and Herrmann, W., 2001. Hydrothermal alteration and volatile element haloes for the Rosebery K lens volcanic-hosted massive sulfide deposit, western Tasmania; Economic Geology, v. 96, p. 1055–1072.

Lentz, D.R. and Goodfellow, W.D., 1993. Petrology and mass balance constraints on the origin of quartz augen schist associated with the Brunswick massive sulphide deposits, Bathurst, New Brunswick; Canadian Mineralogist, v. 31, p. 877–903.

Lentz, D.R. and Goodfellow, W.D., 1996. Intense silicification of footwall sedimentary rocks in the sulphide stringer zone beneath the Brunswick No. 12 massive sulphide deposit,

Bathurst, New Brunswick; Canadian Journal of Earth Sciences, v. 33, p. 284–302.

Lentz, D.R., Hall, D.C., and Hoy, L.D., 1997. Chemostratigraphic, alteration, and oxygen isotope trends in a profile through the stratigraphic sequence hosting the Heath Steele B zone massive sulphide deposit, New Brunswick; Canadian Mineralogist, v. 35, p. 841–874.

Luff, W., Goodfellow, W.D., and Juras, S., 1992. Evidence for a feeder pipe and associated alteration at the Brunswick No. 12 massive sulfide deposit; Exploration and Mining Geology, v. 1, p. 167–185.

MacLellan, K.L., Lentz, D.R., and McClenaghan, S.H., 2006. Petrology, geochemistry, and genesis of the copper zone at the Brunswick No. 6 volcanogenic massive sulfide deposit, Bathurst Mining Camp, New Brunswick, Canada; Exploration and Mining Geology, v. 15, p. 53–76.

McClenaghan, S.H., Goodfellow, W.D., and Lentz, D.R., 2003. Gold in massive sulfide deposits, Bathurst Mining Camp: distribution and genesis, *In:* Massive sulfide deposits of the Bathurst mining camp, New Brunswick, and northern Maine, (ed.) W.D. Goodfellow, S.R McCutcheon, and J.M. Peter; Society of Economic Geologists, Economic Geology Monograph 11, p. 303–326.

McClenaghan, S.H., Lentz, D.R., and Cabri, L.J., 2004. Abundance and speciation of gold in massive sulphides of the Bathurst Mining Camp, New Brunswick, Canada; Canadian Mineralogist, v. 42, p. 851–871.

McClenaghan, S.H., Lentz, D.R., and Beaumont-Smith, C.J., 2006. The gold-rich Louvicourt volcanogenic massive sulfide deposit, New Brunswick: a Kuroko analogue in the Bathurst Mining Camp, *In:* Volcanic-Hosted Massive Sulfide Deposits and their Geological Settings in the Bathurst Mining Camp, New Brunswick, (ed.) D.R. Lentz; Exploration and Mining Geology, v. 15, p. 127–154.

McClenaghan, S.H., Lentz, D.R., Martin, J., and Diegor, J., 2009. Gold in the Brunswick No. 12 volcanogenic massive sulfide deposit, Bathurst Mining Camp, Canada: Evidence from bulk-ore analysis and laser ablation ICP-MS data on sulfide phases; Mineralium Deposita, v. 44, p. 523–557.

McClenaghan, S.H., 2011. Trace-element systematics of volcanogenic massive sulphide deposits in the Bathurst Mining Camp, New Brunswick, Canada: Exploration to petrogenetic implications; Ph.D. thesis, University of New Brunswick, Fredericton, New Brunswick, 664 p.

McLellan, K.L., Lentz, D.R., and McClenaghan, S.H., 2006. Petrology, geochemistry, and genesis of the copper zone at the Brunswick No. 6 volcanogenic massive sulphide deposit, Bathurst Mining Camp, New Brunswick, Canada; Exploration and Mining Geology, v. 15, p. 53–76.

Mireku, L.K. and Stanley, C.R., 2007. Lithogeochemistry and hydrothermal alteration at the Halfmile Lake South Deep Zone, a volcanic-hosted massive sulfide deposit, Bathurst Mining Camp, New Brunswick; Exploration and Mining Geology, v. 15, p. 177–199.

Paton, C., Hellstrom, J.C., Paul, B., Woodhead, J.D., and Hergt, J.M., 2011. Iolite: Freeware for the visualisation and processing of mass spectrometric data; Journal of Analytical Atomic Spectrometry, v. 26, p. 2508–2518.

Peter, J.M., Kjarsgaard, I.M., Goodfellow, W.D., 2003a. Hydrothermal sedimentary rocks of the Heath Steele Belt, Bathurst Mining Camp, New Brunswick: Part 1. Mineralogy and mineral chemistry, *In:* Massive sulfide deposits of the Bathurst mining camp, New Brunswick, and northern Maine, (ed.) W.D. Goodfellow, S.R McCutcheon, and J.M. Peter; Society of Economic Geologists, Economic Geology Monograph 11, p. 361–390.

Peter, J.M., Goodfellow, W.D., Doherty, W., 2003b. Hydrothermal sedimentary rocks of the Heath Steele Belt, Bathurst Mining Camp, New Brunswick: Part 2. Bulk and rare earth element geochemistry and implications for origin, *In:* Massive sulfide deposits of the Bathurst mining camp, New Brunswick, and northern Maine, (ed.) W.D. Goodfellow, S.R McCutcheon, and J.M. Peter; Society of Economic Geologists, Economic Geology Monograph 11, p. 391–416.

Roberts, F.I., 1982. Trace element chemistry of pyrite: a useful guide to the occurrence of sulfide base metal mineralization; Journal of Geochemical Exploration, v. 17, p. 49–62.

Rogers, R., Ross, P.S., Goutier, J., and Mercier-Langevin, P., 2014. Using physical volcanology, chemical stratigraphy, and pyrite geochemistry for volcanogenic massive sulfide exploration: an example from the Blake River Group, Abitibi Greenstone Belt; Economic Geology, v. 109, p. 61–88.

Rose, D.G. and Johnson, S.C., 1990. New Brunswick computerized mineral occurrence database; New Brunswick Department of Natural Resources and Energy, Mineral Resources Division, internal report.

Ryall, W.R., 1981. The forms of mercury in some Australian stratiform Pb-Zn-Ag deposits of different regional metamorphic grades; Mineralium Deposita, v. 16, p. 425–435.

Soltani Dehnavi, A., Lentz, D.R., and McFarlane, C., 2012. New insight into the massive sulfide deposits in the Bathurst Mining Camp, New Brunswick: implication for volatile element signatures like Cd, Sb, Tl, As, and Hg elements in massive sulphide, *In:* Abstracts; Exploration, Mining and Petroleum New Brunswick conference, Fredericton, New Brunswick, November 4–6, 2012.

Soltani Dehnavi, A., McFarlane, C.R.M., McClenaghan, S.H., and Lentz, D.R., 2013a. In situ LA-ICP-MS of sulfide minerals in VMS deposits throughout the Bathurst Mining Camp, New Brunswick, Canada: volatile trace element contents and distribution with implications for their syngenetic to polyphase metamorphic history, *In:* Conference Program and Abstracts volume; Society of Economic Geologists Geoscience for Discovery 2013, Whistler, September 24–27, 2013.

Soltani Dehnavi, A., McFarlane, and Lentz, D.R., 2013b. Sulfide mineral chemistry from the massive sulfide deposits of Bathurst Mining Camp, Canada: implication for volatile trace-elements distribution and developing the trace-element exploration vectoring tool, *In:* Abstracts; Exploration, Mining and Petroleum New Brunswick conference, Fredericton, NB, November 2013.

Soltani Dehnavi, A., Lentz, D.R., McFarlane, C.R.M., and McClenaghan, S.H., 2014a. LA-ICP-MS trace-element study of pyrite from massive sulfide deposits of the Bathurst Mining Camp, Canada: Determination of volatile trace-element contents in pyrite and its application as a vectoring tool for the exploration of VMS deposits, *In:* Program with Abstracts; Geological Association of Canada-Mineralogical Association of Canada Annual Meeting, Fredericton, May 20–22, 2014, p. 260.

Soltani Dehnavi, A., McFarlane, C.R.M., Lentz, D.R., and McClenaghan, S.H., 2014b, Variation in sulphide mineral chemistry in massive sulfide deposits, Bathurst Mining Camp, Canada: Implication for measuring volatile trace-elements by LA-ICP-MS and its application as a vectoring tool for the exploration of VMS deposits, *In:* Program with Abstracts; Geological Association of Canada-Mineralogical Association of Canada Annual Meeting, Fredericton, May 20–22, 2014, p. 259–260.

Soltani Dehnavi, A., Lentz, D.R., and McFarlane, C.R.M., 2014c. Interpreting volatile trace-element signatures in volcanogenic massive sulphide deposits of the Bathurst Mining Camp,

Canada: Evidence from a LA-ICP-MS study on sulfide minerals, *In:* Abstracts; Goldschmidt conference, Sacramento, June 8–13, 2014, p. 2347.

Soltani Dehnavi, A., McFarlane, C.R.M., McClenaghan, S.H., and Lentz, D.R., 2014d. In situ LA ICP-MS of sulphide minerals in VMS deposits throughout the Bathurst Mining Camp, New Brunswick, Canada: volatile trace element contents and distribution with implications for their syngenetic to polyphase metamorphic history; Geological Survey of Canada, Open File 7537. doi:10.4095/293681

Soltani Dehnavi, A., Lentz, D.R., McFarlane, C.R.M., and McClenaghan, S.H., 2014e. In situ LA-ICP-MS systematics for quantitative volatile trace-element measurement in sulfide minerals: from developing methodology to its application in the case study of massive sulfide deposits of the Bathurst Mining Camp, Canada, *In:* Conference Program and Abstracts volume; Exploration, Mining and Petroleum New Brunswick conference, Fredericton, November 2-4, 2014, p. 91.

Soltani Dehnavi, A., McFarlane, C.R.M., Lentz, D.R., and McClenaghan, S.H., 2014f. Variations in phyllosilicate mineral chemistry from the massive sulfide deposits of the Bathurst Mining Camp, Canada: LA-ICP-MS systematics and its application in determination of volatile trace-element suite applicable in VMS exploration, *In:* Conference Program and Abstracts volume; Exploration, Mining and Petroleum New Brunswick conference, Fredericton, November 2-4, 2014, p. 93.

Walker, J.A. and Lentz, D.R., 2006. The Flat Landing Brook Zn-Pb-Ag massive sulfide deposit, Bathurst Mining Camp, New Brunswick, Canada, *In:* Volcanic-hosted Massive Sulfide Deposits and their Geological Settings in the Bathurst Mining Camp, New Brunswick, (ed.) D.R. Lentz; Exploration and Mining Geology, v. 15, p. 99–126.

Walker, J.A. and McCutcheon, S.R., 2011. A chemostratigraphic assessment of core from the discovery hole of the Halfmile Lake Deep VMS Zone, Bathurst Mining Camp, northeastern New Brunswick, *In:* Geological Investigations in New Brunswick for 2010, (ed.) G.L. Martin; New Brunswick Department of Natural Resources, Lands, Minerals and Petroleum Division, Mineral Resource Report 2011-2, p. 1–49.

Wilson, S.A., Ridley, W.I., and Koenig, A.E., 2002. Development of sulfide calibration standards for the laser ablation inductively-coupled plasma mass spectrometry technique; Journal of Analytical Atomic Spectrometry, v. 17, p. 406–409.

Yang, K., Huntington, J. F., Gemmell, J. B., Scott, K. M., 2011. Variations in composition and abundance of white mica in the hydrothermal alteration system at Hellyer, Tasmania, as revealed by infrared reflectance spectroscopy; Journal of Geochemical Exploration, v. 108, p. 143–156.